

# Exchange coupling in transition-metal nano-clusters on Cu(001) and Cu(111) surfaces

Phivos Mavropoulos,\* Samir Lounis, and Stefan Blügel  
*Institut für Festkörperforschung (IFF) and Institute for Advanced Simulation (IAS),  
 Forschungszentrum Jülich, D-52425 Jülich, Germany*

We present results of density-functional calculations on the magnetic properties of Cr, Mn, Fe and Co nano-clusters (1 to 9 atoms large) supported on Cu(001) and Cu(111). The inter-atomic exchange coupling is found to depend on competing mechanisms, namely ferromagnetic double exchange and antiferromagnetic kinetic exchange. Hybridization-induced broadening of the resonances is shown to be important for the coupling strength. The cluster shape is found to weaken the coupling via a mechanism that comprises the different orientation of the atomic  $d$ -orbitals and the strength of nearest-neighbour hopping. Especially in Fe clusters, a correlation of binding energy and exchange coupling is also revealed.

## I. INTRODUCTION

The magnetism of transition metal nanostructures on metallic surfaces has been studied extensively in the past with emphasis on the magnetic moments and ground state magnetic configuration. Sophisticated experimental techniques for preparation, such as mass-selection and soft-landing of free clusters, together with the ability to probe the magnetism of these structures on the atomic scale, e.g. by X-ray magnetic circular dichroism, have considerably advanced the field.<sup>1,2</sup> Strong fluctuations of the magnetic properties have been found as a function of cluster size and shape, position of the individual atoms in the cluster, or geometry of the substrate.<sup>1,2,3,4,5,6,7,8,9,10,11,12</sup> In some cases, though, it has been possible to recognize and interpret regularities, and derive rules of thumb based on an understanding of the electronic structure.

Supported clusters of atoms from the end of the  $3d$ -series (Fe, Co, Ni) are known to be ferromagnetic, due to a double-exchange mechanism. The spin moments in Fe clusters have been found to vary in a regular way, namely the moment of each Fe atom scales down linearly as a function of the number of Fe neighbours.<sup>8,9,10</sup> This nice effect seems to be independent of the substrate, and persists also in FeCo clusters.<sup>12</sup> On the other hand, in pure Co clusters the moment is practically saturated, while in Ni clusters the atomic moments do not seem to correlate with the coordination number.

For V, Cr and Mn clusters, it has been found that the intra-cluster coupling is antiferromagnetic, leading to frustration and non-collinear magnetic order if the substrate provides appropriate geometry (e.g., (111) surfaces).<sup>13,14</sup> However, if the substrate is magnetic, the exchange coupling to the substrate atoms also plays a role and non-collinear magnetism can appear in Cr and Mn clusters or chains on (001) Ni and Fe surfaces.<sup>15,16,17,18</sup>

The magnitude of the exchange coupling in  $3d$  clusters on surfaces has been less studied so-far. This is an important quantity, however, in determining the stability of the ground state and the crossover or blocking temperature. In addition, recent developments in experimental techniques allow to probe the spectrum of mag-

netic excitations, e.g., via inelastic scanning tunneling spectroscopy<sup>19,20,21,22</sup> or spin-polarized scanning tunneling spectroscopy.<sup>23</sup>

From the theory point of view, calculations on supported<sup>10,24</sup> and free-standing<sup>25</sup> transition-metal clusters have shown that the inter-atomic exchange coupling fluctuates strongly with respect of cluster size, shape, or position of the atoms in the cluster. These works motivate an analysis of the local electronic structure effects, in order to obtain a better insight into the driving mechanisms for these fluctuations.

In this paper we perform such an analysis. We present density-functional results on Cr, Mn, Fe, and Co nano-clusters (up to 9 atoms large) of mono-atomic height on Cu surfaces. For the ferromagnetic clusters (Fe and Co) we also consider Cu(111) as substrate, while for the antiferromagnetic ones we restrict our study to collinear magnetism on Cu(001) (Cr and Mn show non-collinear magnetism on Cu(111)). Our focus is on the inter-atomic exchange coupling, where we attempt to find and understand the trends via the details of the electronic structure. It is gratifying that, in some simple geometries, the results can be interpreted in a transparent way within a simple tight-binding model.

## II. METHOD OF CALCULATION

Our calculations are based on density-functional theory within the local density approximation (LDA), as parametrized by Vosko, Wilk, and Nussair.<sup>26</sup> The Kohn-Sham equations are solved in the framework of the full-potential Korringa-Kohn-Rostoker Green-function method (KKR) with exact treatment of the atomic cell shapes,<sup>27</sup> using an angular momentum cutoff of  $l_{\max} = 3$ . The Cu surfaces were modelled by slabs of a finite thickness of 18 atomic layers; in all calculations, the LDA equilibrium Cu lattice parameter (3.51 Å) was used, while structural relaxations were neglected. Within the KKR method, first the Green function of the host (Cu surface) is calculated, while in a second step a Dyson equation is solved for the Green function of the embedded cluster. For all clusters, neighbouring host atoms were considered

in the self-consistent calculation in order to account for the screening of the charge.

The exchange coupling is calculated by the method of infinitesimal rotations.<sup>28</sup> This method is based on a hypothesis of correspondence between the energy change  $\Delta H$  of the Heisenberg Hamiltonian

$$H = - \sum_{nn'} J_{nn'} \hat{e}_n \cdot \hat{e}_{n'} \quad (1)$$

and the total energy change found within DFT,  $\Delta E_{\text{DFT}}$ , upon rotating the magnetic moment directions  $\hat{e}_n$  and  $\hat{e}_{n'}$ . By virtue of the magnetic force theorem this energy change can be calculated by the difference in the Kohn-Sham eigenvalues. One obtains the exchange constants by taking a second derivative,  $J_{nn'} = -\frac{1}{2} \partial^2 H / (\partial \hat{e}_n \partial \hat{e}_{n'}) = -\frac{1}{2} \partial^2 E_{\text{DFT}} / (\partial \hat{e}_n \partial \hat{e}_{n'})$ , as<sup>28</sup>

$$J_{nn'} = \frac{1}{4\pi} \int^{E_F} \text{Im Tr}_{lm} G_{nn'}^\uparrow(E) [t_n^\uparrow(E) - t_{n'}^\downarrow(E)] \times G_{n'n}^\downarrow(E) [t_n^\uparrow(E) - t_{n'}^\downarrow(E)] dE \quad (2)$$

$$= \int^{E_F} j_{nn'}(E) dE \quad (3)$$

where  $G_{nn'}^{\uparrow,\downarrow}(E)$  is the inter-site KKR structural Green function for spin up ( $\uparrow$ ) or down ( $\downarrow$ ),  $t_n^{\uparrow,\downarrow}$  are spin-dependent scattering matrices at sites  $n$  and  $n'$ , and  $\text{Tr}_{lm}$  indicates a trace in angular momentum indices ( $G_{nn'}$  and  $t_n$  are matrices in angular-momentum space). We have also identified the integrand as an “exchange coupling density”  $j_{nn'}(E)$ , which is useful for the analysis of the results. In short, if the moments of two atoms are rotated with respect to each other by a small angle  $\theta$ , then the difference in energy arises primarily due to shifts of the atomic energy levels or resonances. Then,  $\theta^2 j_{nn'}(E)$  gives the energy-shift of the local states at  $E$ , while  $\theta^2 J_{nn'}$  gives the change in total energy; a subtraction of the interaction with the rest of the magnetic atoms is also included implicitly. We also introduce the sum of the exchange interactions in the  $n$ -th atom in the cluster,

$$J_0^{(n)} = \sum_{n'} J_{nn'}, \quad (4)$$

which is a measure of “local spin stiffness”. Integrating  $j$  up to a certain energy  $E$ , instead of  $E_F$ , yields  $J(E)$  and  $J_0(E)$  that also helps to analyze the contribution of specific states.

In practice, the set of equations (1) and (2) is an accurate parametrization of the DFT total energy only for small deviations from a reference state. Usually the ground state is chosen as reference, which can be ferromagnetic or antiferromagnetic. Eq. (2) then yields  $J > 0$  if energy must be paid for mutually rotating the spins direction, and  $J < 0$  if energy is gained. Thus, starting from a ferromagnetic or antiferromagnetic state within the LDA,  $J > 0$  always indicates stability of this state, irrespectively if it is ferro- or antiferromagnetic; the extra ( $-$ ) sign associated with antiferromagnetism in (1) is absorbed, so to say, in either  $\hat{e}_n$  or  $\hat{e}_{n'}$ .

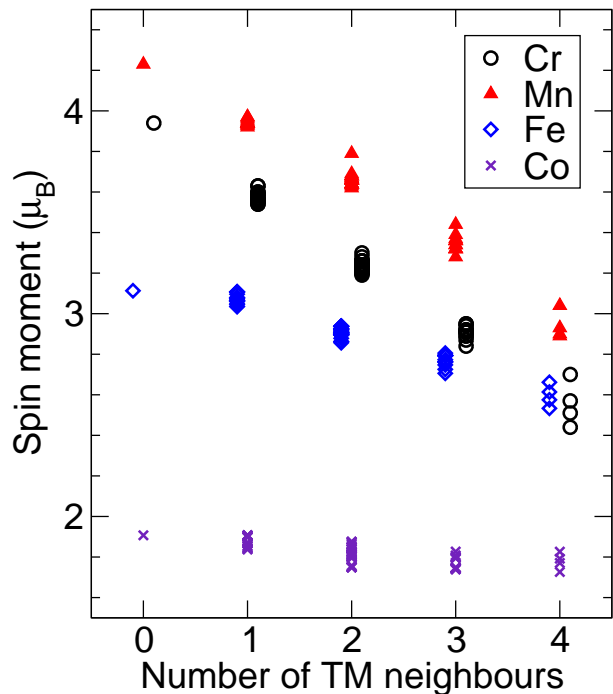


FIG. 1: Atomic spin moment of Cr, Mn, Fe, and Co in corresponding clusters of 14 different cluster geometry types, ranging from 1 to 9 atoms, on the Cu(001) surface. The moment shows a linear trend as a function of the coordination number of nearest transition-metal (TM) neighbours.

### III. ATOMIC SPIN MOMENTS

In Fig. 1 we show the dependence of the atomic moments as a function of neighbouring atoms for Cr, Mn, and Fe, and Co. The strongest atomic spin moments are found, as expected, in Mn clusters, ranging from  $4.23 \mu_B$  for a single adatom to  $2.89 \mu_B$  for the central atom of a 9-atom cluster. Cr shows somewhat lower moments, then comes Fe and finally Co. In a previous paper<sup>8</sup> we showed that the atomic moments  $M$  in Fe drop with increasing coordination following approximately a simple linear relation,

$$M(i) = -aN_c(i) + b, \quad (5)$$

where  $N_c$  is the number of nearest neighbours of the  $i$ -th Fe atom in the cluster and  $a$  and  $b$  are positive constants (independent of  $i$ ). This relation simply expresses the common wisdom that the moment decreases with hybridization, and that the hybridization mainly depends on the number of nearest neighbours. However, this was found not to be so simple for Co, where the moment is more saturated and for Ni.<sup>8</sup> Additional effects come from interference among the  $d$  states of remote atoms in the cluster, at the onset of a narrow  $d$ -band formation at the Fermi level  $E_F$ , giving a stronger relative scatter to the data.

In the case of Cr and Mn clusters, relation (5) holds

rather well (here for the absolute value of  $M$ , since the clusters are antiferromagnetic). As the  $d$ -states of these elements are either below the Fermi level (for majority-spin) or above the Fermi level (for minority-spin), there is no  $d$ -band formation at  $E_F$  (see Fig. 2 for the density of states of Cr, Mn, Fe, and Co dimers). In addition, the antiferromagnetic configuration allows for  $d$ - $d$  hybridization only between occupied and unoccupied states making it comparatively weak, which is reflected on the smooth, Lorentzian-like, minority-spin density of states, contrary to Fe and Co. (The majority-spin resonances appear wider in Mn, Fe, and Co, because of their interaction with the Cu substrate  $d$ -band that lies at approximately the same energy.) Since the hybridization at  $E_F$  arises primarily due to the extended  $s$  states of the first neighbours, the behavior of the moments correlates smoothly with the coordination. In the case of Co, the moment is almost saturated, changing very little with coordination; the fluctuation in  $M$  cannot be correlated to  $N_c$ . The weak scatter of data for any particular coordination corresponds to different atoms on different clusters.

#### IV. EXCHANGE COUPLING: PRELIMINARY REMARKS

We proceed with the exchange coupling in the nano-clusters. Before presenting the density-functional results, we discuss how one can interpret these in terms of a simple model.

The inter-atomic exchange coupling depends on various factors. The nearest-neighbour exchange can be interpreted in terms of the local density of states (DOS). The longer-range interactions, on the other hand, are governed by a generalization of the Ruderman-Kittel-Kasuya-Yosida (RKKY) interaction,<sup>29</sup> depend on the properties of the Fermi surface, and are far more complex in nano-clusters, as a Fermi surface is not yet formed. Also, details of the surroundings of the cluster can play a role due to quantum confinement.<sup>30</sup> Furthermore, the substrate below the surface layer, e.g. buried magnetic clusters or layers,<sup>31</sup> can affect the long-range interactions; even non-magnetic buried structures can play a role as spin-dependent wavefunctions incident from a magnetic atom at the surface can be reflected at the buried structure and propagate to another atom back on the surface, especially in the presence of Fermi-surface focusing.<sup>32</sup> Another type of exchange interaction is the anisotropic exchange of the Dzyaloshinskii-Moriya type, which has been found, for example, to produce a long-wavelength, non-collinear magnetic ground state in Mn overlayers on W(110).<sup>33</sup> This, however, depends on the spin-orbit coupling, and even in transition-metal clusters on Au and Pt (where the spin-orbit coupling is strong), the anisotropic exchange is found to be two orders of magnitude weaker than the nearest-neighbour Heisenberg exchange.<sup>34,35</sup> In Cu, spin orbit coupling is much weaker, therefore we consider that its effect can be safely neglected for the small-

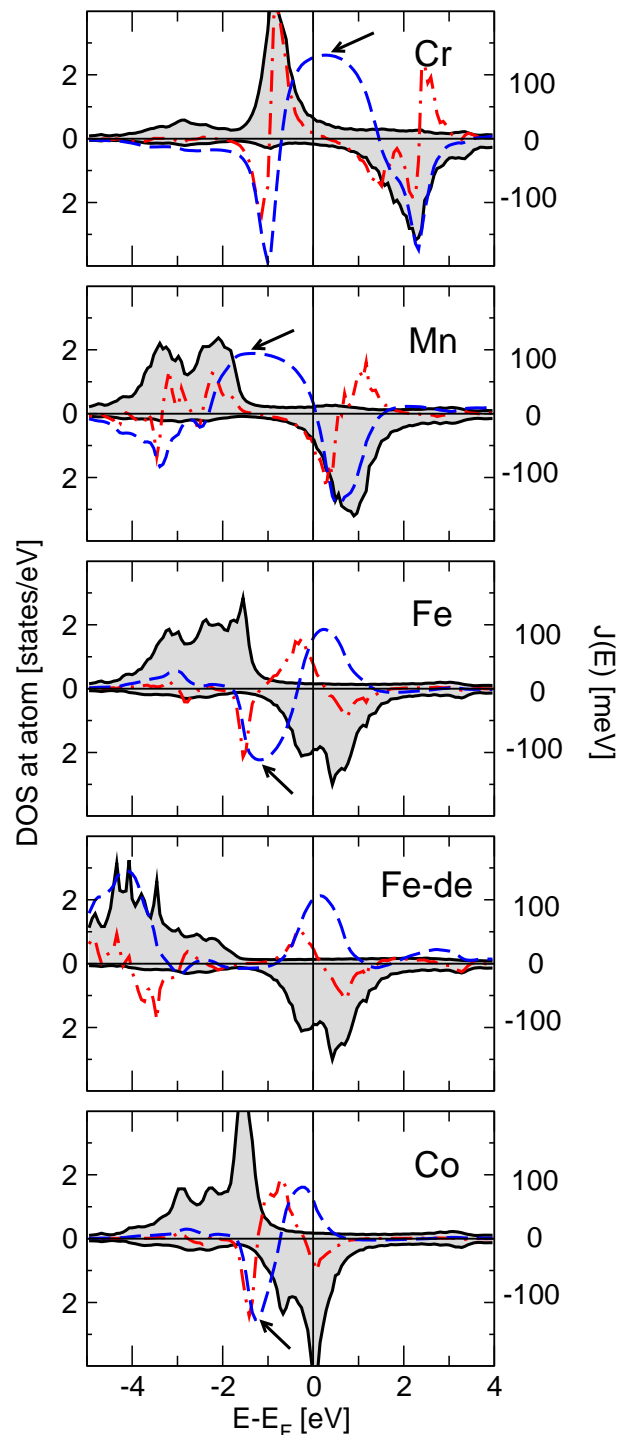


FIG. 2: Density of states and exchange coupling for Cr, Mn, Fe, and Co dimers on Cu (001). Label “Fe-de” corresponds to a Fe dimer with the majority states pushed to low energies, so that the double exchange becomes evident. Full, black line over shaded area (left scale): density of states; upper panels correspond to majority spin, lower panels to minority spin. Dashed, blue line (right scale): exchange coupling  $J(E) = \int^E j(E')dE'$  as a function of energy;  $J(E_F)$  corresponds to the actual exchange constant. Arrows indicate the particular local maxima of  $J(E)$  that correspond to the kinetic-exchange mechanism (absent in the “Fe-de” case, where both maxima of  $J(E)$  correspond to the double-exchange mechanism). Dashed-dotted red line: exchange density  $j(E)$  (not to scale).

size clusters that we examine here. Following these considerations, we focus our discussion only on the nearest-neighbour Heisenberg-type exchange coupling, which is also much stronger than more-distant interactions.

As is long known,<sup>36</sup> there are two main contributions to  $J$ , of different origin: the first, sometimes called “kinetic exchange”, favours antiferromagnetism in Cr and Mn. The second, sometimes called “double exchange”, favours ferromagnetism in Co and Fe. Both mechanisms are associated with direct hopping among  $d$  states of neighbouring atoms. As we will see below, the two mechanisms can be present simultaneously and compete, reducing the absolute value of  $J$ .<sup>37</sup>

To proceed with the discussion, consider two neighbouring transition metal atoms. *Kinetic exchange* arises from a level repulsion between occupied majority states of an atom with unoccupied minority states of a neighbouring atom, when the moments of the two are oppositely oriented. In a simple tight-binding picture, let us assume that the energy of the occupied  $d$  level is at  $E_d - \Delta < 0$ , while the unoccupied level is at  $E_d + \Delta > 0$ , where  $2\Delta$  is the exchange splitting; the Fermi energy is assumed to be at  $E_F = 0$ . Allowing for a hopping  $t$  between two neighbouring atoms, the levels move to  $E_{\pm} = E_d \pm \sqrt{\Delta^2 + t^2}$ . Upon forcing the two moments to a ferromagnetic configuration, the shift vanishes and the occupied levels move higher, which costs energy  $2[(E_d - \Delta) - E_-] = 2(\sqrt{\Delta^2 + t^2} - \Delta) \approx t^2/\Delta$ , for  $\Delta \gg t$  (the factor 2 accounts for the number of occupied states). This picture does not change even in the presence of a broadening by a hybridization  $\Gamma$  of the levels with a background continuum (as long as the broadened resonance does not cross  $E_F$ ), since the center-of-mass of the  $d$  levels is normally not shifted by  $\Gamma$ .

*Double exchange* arises if the majority-spin or minority-spin states of the two transition metal atoms are in the proximity of  $E_F$ , i.e., either  $E_d - \Delta \approx 0$  or  $E_d + \Delta \approx 0$ . Suppose that the two moments are ferromagnetically oriented, and that  $E_d + \Delta = 0$ . Allowing for a hopping  $t$  between the  $d$ -states, the minority levels split into bonding and antibonding, and are driven to  $E_{\pm} = \pm t$ ;  $E_-$  is occupied,  $E_+$  empty. Upon forcing the two moments to an antiferromagnetic configuration, the splitting vanishes, and the occupied  $E_-$  move back to  $E_F$ . This costs energy  $t$ . (The same splitting occurs also for the majority levels, but does not affect the total energy as they are fully occupied and their center-of-mass does not change). The energy gained by the double-exchange mechanism, however, is reduced if the  $d$ -states are resonant with a background hybridization  $\Gamma$ , because the tails of the bonding and antibonding resonances cross  $E_F$ , so that their repopulation partly counter-acts the energy gain. A simple calculation shows that the energy gain by the hopping,  $\int_{-\infty}^0 E \Delta n(E) dE$ , is a decreasing function of  $\Gamma$  ( $\Delta n(E)$  is here the difference between the density of states without and with hopping, and only the single-particle energies are considered).

Now, if the double-exchange mechanism is present, it

must coexist with kinetic exchange, which cannot be switched off. There is then a competition between the two, and in the simple picture given above (disregarding the hybridization), the criterion for a ferromagnetic ground state is  $t > t^2/\Delta$ , i.e.  $\Delta > t$ . Otherwise the ground state is antiferromagnetic. This analysis also suggests a way to reveal the strength of the double-exchange mechanism in a calculation, which we use below. If the majority-spin states are artificially driven to lower energies by acting on them with an attractive potential, the kinetic exchange  $t^2/\Delta$  will decrease and what is left will be mainly the double exchange part.

To conclude this subsection, nearest-neighbour exchange coupling can partly be understood in terms of bond formation, but there are competing factors that decide its final value.

## V. EXCHANGE COUPLING: RESULTS AND DISCUSSION

We now present and analyze the exchange coupling calculated within density-functional theory. Results on most of the investigated clusters are shown in Fig. 3. As we expected, we find an antiferromagnetic coupling for Cr and Mn clusters, dominated by kinetic exchange, while Fe and Co are ferromagnetic, dominated by double exchange. On the average, the interaction strength decreases with increasing cluster size, dimers showing the strongest coupling, but there are many exceptions (especially for Mn), while the local geometry around each atom plays a role.

Cr is the champion in the strength of exchange coupling, with values as high as  $|J| = 134$  meV for the Cr/Cu(001) dimer. Mn clusters show comparatively weak coupling: for the Mn/Cu(001) dimer we find  $|J| = 28$  meV, a value which increases by up to 70% for certain configurations. In Fe the coupling is again strong, reaching  $J = 81$  meV for the Fe/Cu(001) and 100 meV for the Fe/Cu(111) dimer. In Co, finally, the coupling is again relatively weaker, reaching values of  $J = 68$  meV for the Co/Cu(001) and 80 meV for the Co/Cu(111) dimer. We proceed with an analysis of our results based on the model that were presented in the preceding section.

### A. Dimers: exchange coupling and density of states

In a first step, we discuss the exchange coupling in dimers on Cu(001) and relate it to the electronic structure. The picture that is derived here is helpful in understanding the behavior of larger clusters.

Our guide for the discussion is Fig. 2. There, the density of states is shown for one of two atoms of a Cr, Mn, Fe, and Co dimer (the other atom has exactly the same DOS, but for Cr and Mn the spin directions are interchanged). In the same figure, the energy-dependent

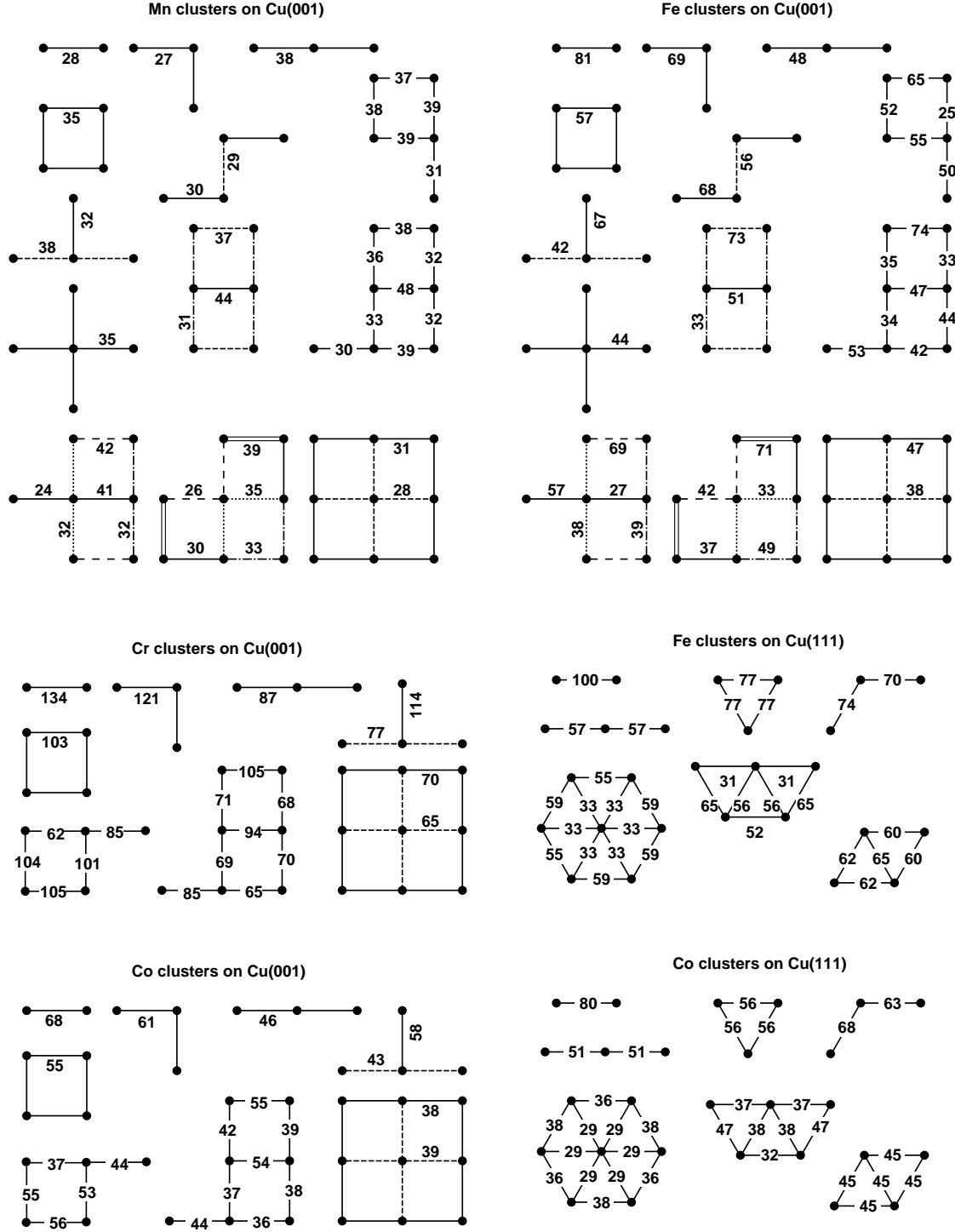


FIG. 3: Nearest-neighbour exchange coupling (absolute value, in meV) for Cr, Mn, Co, and Fe nano-clusters on Cu(001) and Cu(111). A schematic top-view of the clusters is shown, the Cu surface is understood to be one atomic layer below. The view corresponds to surface-adapted geometry, i.e., rotated with respect to the fcc cubic axes by  $45^\circ$ . Coupling values identical by symmetry are not annotated more than once, but indicated by the same line-type (e.g., full or dashed line). For Co/Cu(001), Cr/Cu(001), and Fe and Co/Cu(111), only selected clusters are shown. On the (111) surface, couplings that appear on first sight equivalent by symmetry can differ, due to the relative displacement of the sub-surface layer.

exchange coupling density,  $j(E)$ , and coupling,  $J(E) = \int^E j(E')dE'$ , are shown (see Eq. 3).

In all cases, the majority- and minority-spin  $d$ -resonances can be clearly seen. Around each resonance,  $j(E)$  (dash-dotted red line) shows an S-shaped form, revealing the change of the resonance form upon rotating the spins with respect to each other. In Cr and Mn, the lower levels of each resonance will move even lower and the higher levels will move higher: the resonance will widen up. This is because the starting point is here an antiferromagnetic orientation of the moments, and rotation allows for majority-majority and minority-minority hopping. In Fe and Co, where the starting point is a ferromagnetic orientation, the opposite will happen: the resonance will narrow down, because majority-majority and minority-minority begins to be blocked; thus, the S-shape is inverted. As the minority spin resonance is bisected by  $E_F$  for Fe and Co, the single-particle part of the energy,  $\int^{E_F} E n(E) dE$ , will increase, signalling a ferromagnetic coupling of the double-exchange type. Note that the behaviour of  $j(E)$  is more spiked at the majority resonance in Mn and Fe, due to the hybridization with the Cu  $d$ -states; moreover, in Cr, Mn, and Fe the shape of  $j(E)$  around the minority-spin resonance appears to have a double-S form, revealing contributions from different  $d$ -orbitals at slightly different energies. Around the S-shapes, the integral  $J(E)$  shows peaks (positive or negative, depending on the starting moment configuration) revealing the total strength of the interaction.

At some energy between the resonances,  $j(E)$  passes through zero; however,  $J(E)$  can show a plateau with a local maximum at those energies. This reveals a net shift of the resonances, apart from the broadening or narrowing, upon rotation of the moments. The net shift stems from the majority-minority-state repulsion, and can be identified with the kinetic exchange. Its maximal value, indicated by arrows in Fig. 2, is strong in Cr, but less so in Mn, probably because the Mn  $d$ -states are lower in energy and thus more localized spatially, reducing the hopping. This is one reason why Mn shows a weaker exchange coupling than Cr. Another, more important reason is that for Cr  $E_F$  bisects  $J(E)$  at a high point, in the middle of the plateau, while for Mn  $E_F$  is already at a point strong descent of  $J(E)$ , close to changing sign. Here, the double-exchange mechanism among the minority-spin states is already starting to set in, competing with the kinetic exchange.<sup>38</sup> This affects the behaviour of the coupling with increasing cluster size, as we discuss later.

The kinetic exchange is also present for Fe and Co; it is just that double-exchange is stronger and dominates, causing a ferromagnetic ground state. It is interesting to disclose the strength of the double-exchange by shifting the majority-spin resonances of Fe and Co to lower energies, so that the kinetic exchange is diminished. We achieved this by acting on these states with an attractive potential of 2.7 eV. This resulted in an increase of the coupling by approximately 50% for all Fe and Co clusters. An energy-resolved picture of this can be seen in the

case of a Fe dimer, the DOS of which is shown in Fig. 2, labelled “Fe-de”. Here,  $J(E)$  does not show a peak between the resonances any more (the kinetic exchange is now absent), while it is bisected by  $E_F$  much closer to its maximum than in the normal Fe dimer.

## B. Trimers: the role of local geometry

Having discussed the exchange in dimers, we now focus on the complications brought about by local geometry effects. These can be best demonstrated in the example of trimers, since for larger clusters there are too many parameters that play a role.

We begin with an observation. The exchange coupling in linear trimers is weaker than in corner-shaped ones (see Fig. 3). This is true for Cr/Cu(001), Fe and Co on Cu(001) and Cu(111), but not for Mn/Cu(001). This behavior can be interpreted again in terms of a tight-binding model, but with more than one orbitals. We will do so, deferring the explanation of the Mn to a later point in this subsection.

In the interaction causing the kinetic or double exchange, not all  $d$  orbitals take part equally. Some can have an orientation not favouring bonding, while others can be pointing directly into the neighbouring atom. Consider for instance a linear-shaped trimer in the  $y$ -direction, setting for definiteness the  $x$  and  $y$  axes in the surface plane (schematic positioning of atoms 1, 2, 3 in Fig. 4c). The  $d_{xy}$ ,  $d_{yz}$ , and  $d_{x^2-y^2}$  orbitals point partly toward the neighbour atoms and can hybridize with their counterparts there. The  $d_z$  orbitals point out-of-plane, and can therefore hybridize only weakly with  $d_{x^2-y^2}$  neighbouring orbitals (hybridization with the rest is forbidden by symmetry, if one disregards the surface-induced symmetry breaking in a first approximation). Finally, the  $d_{xz}$  orbitals point away from the neighbours, and are practically non-bonding. Thus three channels have a major contribution to the exchange coupling: one consists of the three  $d_{xy}$  orbitals, one stems from the three  $d_{yz}$ , and one from the three  $d_{x^2-y^2}$ . Because each of these channels is brought about by three orbitals, we call them “triple channels” henceforth. If the trimer were to be extended to a linear chain, these three triple channels would form the most dispersive  $d$  bands.

Now let us change the picture to a corner-shaped trimer (schematic positioning of atoms 1, 2, 3 in Fig. 4d). Here we have only two triple channels, namely the  $d_{x^2-y^2}$  and the  $d_{xy}$  channels where all atoms participate. However, we also have two bonds:  $d_{yz}$ - $d_{yz}$  between atoms 1 and 2, and  $d_{xz}$ - $d_{xz}$  between atoms 2 and 3. In effect, compared to the linear trimer, one triple channel has been replaced by two bonds.

A straightforward calculation shows that the energy gain of two simple bonds is larger than the one of a triple channel. Considering first the case of double exchange, assume that the majority-spin  $d$  levels of the three atoms lie at  $E_d + \Delta = E_F = 0$ . In the linear trimer, if we open

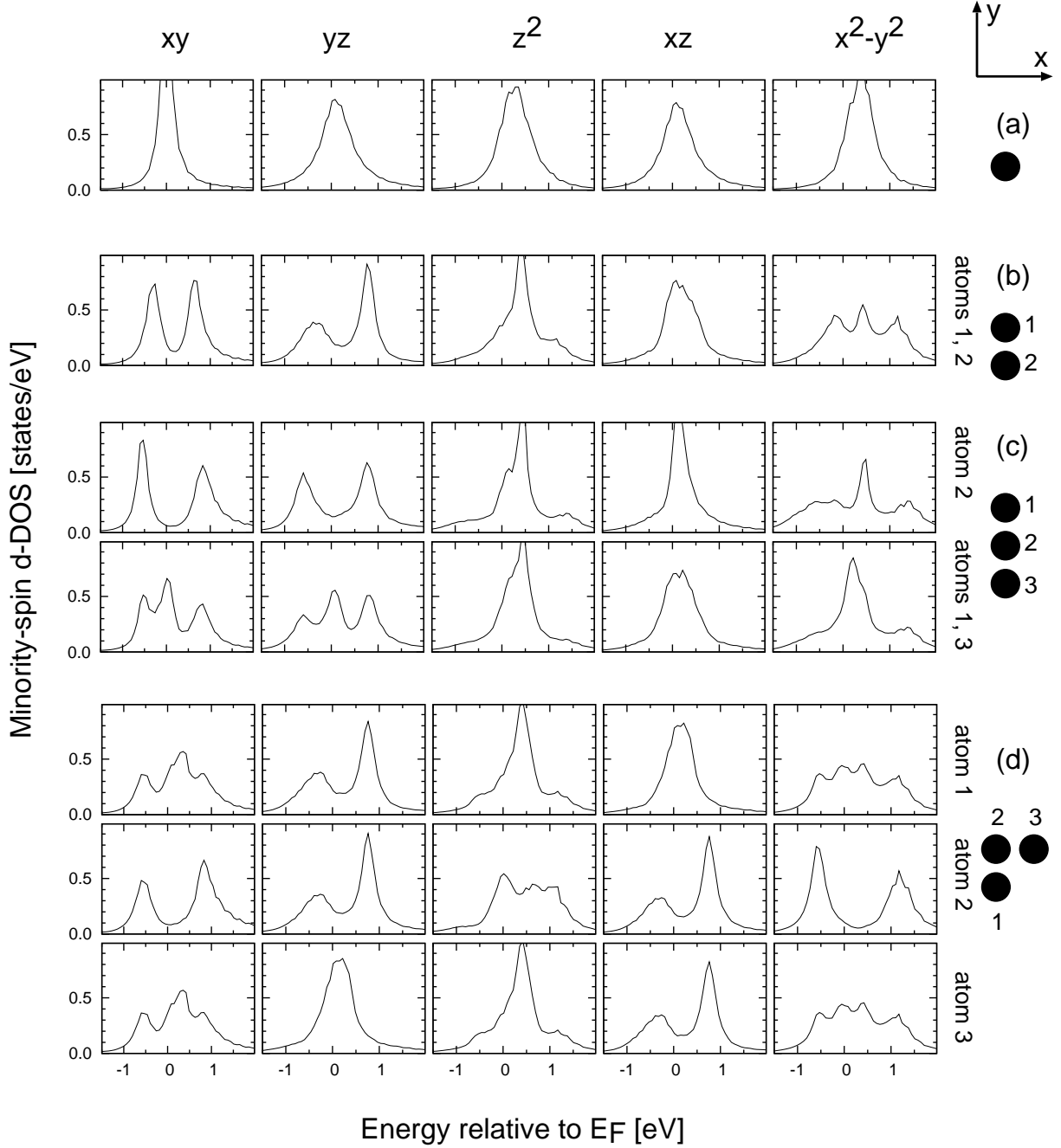


FIG. 4:  $d$ -density of states resolved in  $m$  for a Fe monomer (a), dimer (b), linear trimer (c) and corner-shaped trimer (d). The resonance splittings determine the energy gain from the ferromagnetic state formation.

a triple channel through the  $d_{yz}$  states by allowing for a hopping  $t$ , a threefold splitting is created with  $E_{\pm} = \sqrt{2}t$ ,  $E_0 = 0$ ; the  $d_{xz}$  orbitals are not affected. At half-filling of the minority-spin orbitals (optimal case for double-exchange), the energy gain is  $\Delta E_{\text{tot}}^{\text{Linear}} = \sqrt{2}t$ . In the corner-shaped trimer, allowing a hopping between  $d_{yz}$ - $d_{yz}$  of atoms 1 and 2 and  $d_{xz}$ - $d_{xz}$  of atoms 2 and 3 creates two double splittings of  $E_{\pm} = t$ . Now, at half-filling of the

minority-spin orbitals, the energy gain is  $\Delta E_{\text{tot}}^{\text{Corner}} = 2t$ . Evidently,  $\Delta E_{\text{tot}}^{\text{Corner}} > \Delta E_{\text{tot}}^{\text{Linear}}$ . Carrying out the calculation for the kinetic-exchange case at full majority-spin and empty minority-spin orbitals gives  $\Delta E_{\text{tot}}^{\text{Linear}} = 2(\sqrt{\Delta^2 + t^2} - \Delta)$ ,  $\Delta E_{\text{tot}}^{\text{Corner}} = 4(\sqrt{\Delta^2 + t^2} - \Delta)$ , i.e., again  $\Delta E_{\text{tot}}^{\text{Corner}} > \Delta E_{\text{tot}}^{\text{Linear}}$ . In both cases, the linear trimer should show a smaller exchange  $J$  than the corner-shaped one. Note that no second-neighbour hopping is

necessary in this interpretation. On the (111) surface, the corner-shaped trimer is not in a  $\phi = 90^\circ$  configuration, but rather at  $\phi = 60^\circ$  or  $\phi = 120^\circ$ . Then the effect is still present, but to a lesser extent as the hoppings satisfy partially a triple channel and partially a bond (the hopping contributing to the triple channel is  $t \cos \phi$ , the one contributing to the bond is  $t \sin \phi$ ).

This simple picture can be recognized in the  $m$ -resolved density of  $d$ -states. In Fig. 4 we show the minority-spin  $d$ -DOS for a Fe/Cu(001) adatom, dimer, linear and corner-shaped trimer. In panel (a), among the resonances of the single adatom,  $d_{xy}$  and  $d_{x^2-y^2}$  are clearly the most localized, as the lobes of these orbitals extend mainly in-plane. Upon adding a neighbouring Fe atom (panel b), clear-cut splittings are formed for all orbitals that point toward the Fe neighbour. Even the  $d_{z^2}$  orbital hybridizes somewhat with the  $d_{x^2-y^2}$  of the neighbour, causing a three-peak structure in  $d_{x^2-y^2}$ . Only the  $d_{xz}$  orbital remains oblivious to the presence of the second atom, as it points in the wrong direction and is orthogonal to any neighbouring orbital pointing in its way.

Next we add a third atom to form a linear trimer (upper and lower panel c). Here, more splittings appear. In the two outmost atoms, 1 and 3, orbital  $d_{xy}$  shows now a threefold splitting, corresponding to the three levels  $E_\pm$  and  $E_0$  that are formed within a triple channel, as we discussed above; the same is true for  $d_{yz}$ . This is the onset of band formation. However, the state corresponding to  $E_0$  has no weight in the middle atom, which can also be verified by solving the associated  $3 \times 3$  system of equations within the tight-binding model. For the  $d_{x^2-y^2}$  orbitals the picture is more complicated due to their additional hybridization with  $d_{z^2}$ .

Finally, we move one atom to form a corner-shaped trimer (panel d). Here the  $d_{yz}$  triple channel is broken. Instead, we have a bond between the  $d_{xy}$  of atoms 1 and 2, and an identical bond between the  $d_{xz}$  of atoms 2 and 3. The splittings, looking exactly like the  $d_{yz}$  splitting of the dimer of panel (b), verify this picture. We conclude that the tight-binding model indeed interprets the calculated DOS and coupling in Fe and Co.

We turn now to the interpretation of the behavior of Cr and Mn. For Cr, which is a kinetic-exchange system, it is not the level splittings but the level repulsion that causes the  $90^\circ$ , corner-shaped configuration to show a stronger coupling than the linear configuration, as outlined above. Mn, on the other hand, where the competition of kinetic and double exchange is important, behaves differently. Upon going from the linear trimer to the corner-shaped one, *both* the kinetic and the double exchange are strengthened. Apparently, however, the enhancement of the latter is stronger, so that, in the end, they sum up to a weaker antiferromagnetic coupling.

To conclude this subsection, a simple, nearest-neighbour tight-binding model can be used to qualitatively interpret many of the features of the DOS in dimers and trimers. This supports the interpretation of the exchange coupling that we developed earlier, without

a need to introduce second-neighbour corrections; such corrections are of course always present, but apparently not of central importance. The complications of local geometry effects are revealed and explained in the case of trimers; in particular it becomes clear that very important for the behavior is not only the homogeneous broadening of the resonances, but also the onset of band formation creating geometry-dependent splittings. If the moments are tilted away from parallel orientation, these energy-gaining splittings will start closing up, giving rise to the exchange coupling. We now proceed to the discussion of the exchange in larger clusters.

### C. Increasing size: effect of hybridization

Except for the case of Mn, increasing cluster size leads to weaker coupling. This effect is coming from the stronger hybridization with increasing coordination. For Fe and Co, hybridization contributes to the lowering of exchange coupling in two ways. First, the double-exchange interaction is weakened, as we described in section IV. Second, the tendency for magnetism is weakened, as reflected also in the reduction of the atomic moments of Fe.

For Cr clusters, which are a kinetic-exchange systems, mainly the latter effect should play a role, since kinetic exchange should depend on the splitting but not on the hybridization, as we argued in section IV. However, for this argument it was hypothesized that the resonance does not cross  $E_F$ , which is not completely true here. As one can see from the density of states (Fig. 2), the resonances do cross  $E_F$  to an extent that increases with hybridization (reflected also in the decrease of the Cr moments). Thus the repopulation of the resonance tails also contributes to the weakening of the kinetic exchange.

The effect of hybridization becomes clearer if one compares the values of the exchange coupling on Cu(001) to the ones on Cu(111). In the former case, each atom in the cluster has four Cu neighbours, in the latter only three. We see that, on the average, the coupling on Cu(001) is indeed weaker than on Cu(111) (for the same number of transition-metal neighbours). Further evidence comes from examining Fe and Co clusters on Ni(001) and (111) surfaces (not shown here in detail). Here, additional background hybridization is induced on the one hand from the Ni  $d$  states at  $E_F$  and on the other hand from the smaller lattice parameter. Although the moments, assisted by the ferromagnetic substrate, are slightly larger than on Cu,<sup>8</sup> the exchange coupling within the cluster is significantly weaker, by a factor of up to 50% for Fe/Ni(001) compared to Fe/Cu(001), 40% for Fe/Ni(111) compared to Fe/Cu(111), and 25% for Co/Ni(001) compared to Co/Cu(001).

It is also interesting to compare the systems Co/Pt(111) to Co/Au(111), calculated by Šipr et al.<sup>10</sup> In order to eliminate the effect of increased lattice parameter, Šipr et al. also calculated Co/Au(111) in the

lattice parameter of Pt. Although the Pt substrate is polarizable, enhancing the moments of Co/Pt compared to Co/Au, the pair exchange coupling is weaker for Co/Pt dimers and trimers, compared to the same formations on Au.<sup>39</sup> This effect could be due to the strong hybridization of the Co  $d$  states with the Pt  $d$  bands at  $E_F$  (the  $d$  bands of Au are considerably lower). For larger clusters, however, this trend is not so clear and depends on the local geometry. Additional evidence on the effect of hybridization comes from calculations of Co ad-clusters on Pt(111) in Ref. 24 where it is found that the nearest-neighbour exchange of Co atoms at the cluster surface are larger by approximately a factor 2 compared to interactions of a central Co atom.

Finally we comment on the irregular behaviour of Mn clusters. The irregularity arises from the competition of the kinetic and double exchange analyzed in the discussion on the dimers above, and we also saw it in the case of trimers. Small changes in the electronic structure, caused e.g. by local geometry effects or cluster size, can shift the turning point of  $J(E)$  up and down in energy, disturbing the delicate balance between kinetic and double exchange. This is the reason that the Mn clusters show a rather irregular behavior in  $J_{nn'}$ . More to this point, increasing coordination and hybridization will suppress the double-exchange mechanism stronger than the kinetic exchange, as we discussed in Sec. IV. Therefore, the exchange coupling tends to increase with size in Mn clusters, opposite to Cr, Fe, and Co.

#### D. Correlation of exchange and formation energy

As we discussed so-far, level splittings and shifts are responsible for the nearest-neighbour exchange coupling. However, it is also known that such splittings are contributing to the binding energy. Particularly for  $d$ -states, this idea dates back at least to the model of Friedel for the cohesive energy of transition metals. Therefore, there could be a correlation between the energy gain upon attaching an atom to a cluster and the exchange coupling of this atom with its neighbours. However, other factors also enter the formation energy, and they could outweigh the effect of the  $d$  states.

Of course there is a trivial correlation, in the sense that the total exchange coupling energy of an atom increases with the number of neighbours, and so does its binding energy. What we mean here is a correlation even for atoms of the same coordination. To be more precise, we are looking for a linear relation, of the form

$$E_b(n) = A \sum_{n'} J_{nn'} + E_{\text{rest}} \quad (6)$$

where  $E_b(n)$  is the binding energy of the  $n$ -th atom to the rest of the cluster and  $A$  and  $E_{\text{rest}}$  are constants.

In fact we do find such a correlation for Fe/Cu(001) and Fe/Cu(111), but not for Cr, Mn, or Co (apart from

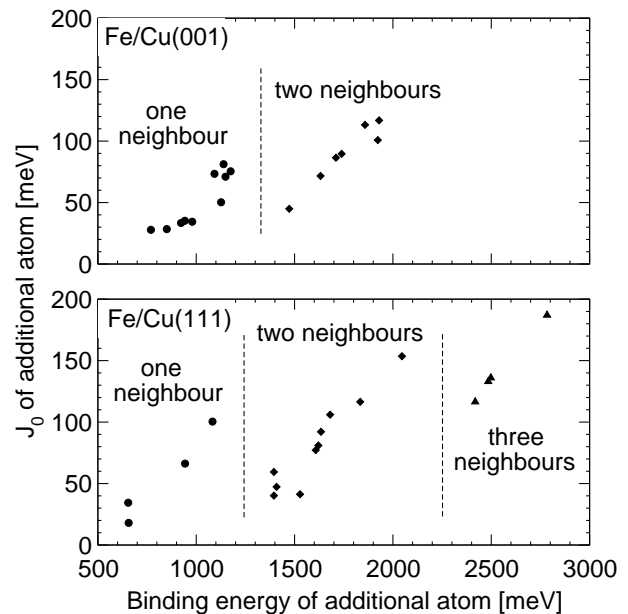


FIG. 5: Correlation between binding energy  $|E_b|$  of a Fe atom to a Fe cluster on Cu(001) and Cu(111) vs. exchange coupling  $J_0$  of the atom to the cluster. Dashed lines indicate the separation between atoms with one, two and three Fe neighbours.

the trivial one mentioned above). We calculate the binding energy  $E_b = E_{N+1} - (E_N + E_{\text{ad}})$ , where  $E_N$  is the total energy of an  $N$ -atom cluster,  $E_{N+1}$  the total energy of the same cluster augmented by one atom, and  $E_{\text{ad}}$  the total energy of a lone-standing adatom (total energies are calculated with respect to the reference energy of the clean Cu surface).

In Fig. 5 we show the relation between the absolute value of the binding energy of cluster atoms,  $|E_b(n)|$ , and the total exchange coupling of these atoms to the rest of the cluster,  $J_0^{(n)} = \sum_{n'} J_{nn'}$ . We only show results for atoms at the cluster edge, as we consider it unlikely that a cluster will be formed with an atom missing in the middle; therefore the maximal number of neighbours is 3. We see a clustering of the data according to the number of neighbours of the added atom, as expected, but within each of these groups, a correlation of the form (6) is evident. There is also a clear “background” coupling, termed  $E_{\text{rest}}$  in relation (6), which varies with the number of neighbours. Deviations from relation (6) can be caused by several effects, such as participation of the  $s$  electrons in the bonding, charge relaxation, moment relaxation (which is rather strong for Cr and Mn), etc. In addition, in the case of Mn, Fe and Co, double exchange and kinetic exchange compete in the final value of  $J_{nn'}$ , while the level shifts associated with kinetic exchange do not contribute to the binding energy for Fe and Co, and the shifts associated with double exchange do not contribute to binding in Mn.

## VI. CONCLUSIONS

The exchange coupling in supported transition metal nano-clusters shows strong fluctuations, depending on cluster size, shape, and position of the atoms in the cluster. Nevertheless, trends can be observed, and the coupling can be analyzed and understood with respect to simple physical terms, namely ferromagnetic double-exchange, antiferromagnetic kinetic exchange, hybridization of the  $d$ -states, and orientation of the  $d$ -orbitals. As these mechanisms act in parallel, they interfere and compete, giving at the end a complex and seemingly irregular picture. It becomes then difficult to isolate the mechanisms in experiment for a direct testing of the theory.

We found that the physical picture and the trends become much more transparent in simple cases, e.g., when studying dimers or trimers of various configurations. We believe therefore that best insight can be gained by studying highly-symmetric, low-dimensional structures, where

only one or two parameters define the structure. Such could be, for instance, linear vs. corner-shaped trimers, or linear vs. zig-zag chains with varying length. As there is considerable progress in experimental techniques for preparation and probing of such structures, a detailed and direct comparison with theoretical results should be possible in the near future.

## Acknowledgments

We are indebted to Ondrej Šipr for sending us detailed results on the Co/Au and Co/Pt systems, and to Peter Dederichs and Yuriy Mokrousov for enlightening discussions. Financial support from the Deutsche Forschungsgemeinschaft (DFG), within the Priority Programme “Clusters in contact with surfaces: electronic structure and magnetism” (SPP-1153), is gratefully acknowledged.

- 
- \* Electronic address: Ph.Mavropoulos@fz-juelich.de
- <sup>1</sup> J.T. Lau, A. Föhlich, R. Nietubyc, M. Reif, and W. Wurth Phys. Rev. Lett. **89**, 057201 (2002).
  - <sup>2</sup> P. Gambardella, S. Rusponi, M. Veronese, S.S. Dhesi, C. Grazioli, A. Dallmeyer, I. Cabria, R. Zeller, P.H. Dederichs, K. Kern, C. Carbone, and H. Brune, Science **300**, 1130 (2003).
  - <sup>3</sup> K. Wildberger, V.S. Stepanyuk, P. Lang, R. Zeller, and P.H. Dederichs, Phys. Rev. Lett. **75**, 509 (1995); V.S. Stepanyuk, W. Hergert, K. Wildberger, S. K. Nayak, and P. Jena, Surf. Sci. **384**, L892 (1997); V. S. Stepanyuk, W. Hergert, P. Rennert, B. Nonas, R. Zeller, and P. H. Dederichs, Phys. Rev. B **61**, 2356 (2000).
  - <sup>4</sup> V. S. Stepanyuk, W. Hergert, P. Rennert, K. Wildberger, R. Zeller, and P. H. Dederichs, Phys. Rev. B **59**, 1681 (1999).
  - <sup>5</sup> J. Izquierdo, A. Vega, L. C. Balbas, D. Sanchez-Portal, J. Junquera, E. Artacho, J. M. Soler, and P. Ordejon, Phys. Rev. B **61**, 13639 (2000);
  - <sup>6</sup> D. Spišák and J. Hafner, Phys. Rev. B **65**, 235405 (2002); Claude Ederer, Matej Komelj, and Manfred Fähnle, Phys. Rev. B **68**, 052402 (2003); A. B. Shick, F. Máca, and P. M. Oppeneer, Phys. Rev. B **69**, 212410 (2004).
  - <sup>7</sup> B. Lazarovits, L. Szunyogh, and P. Weinberger, Phys. Rev. B **65**, 104441 (2002).
  - <sup>8</sup> P. Mavropoulos, S. Lounis, R. Zeller, and S. Blügel, Appl. Phys. A **82**, 103 (2006).
  - <sup>9</sup> J. Hafner and D. Spisak, Phys. Rev. B **76**, 094420 (2007).
  - <sup>10</sup> O. Šipr, S. Bornemann, J. Minár, S. Polesya, V. Popescu, A. Simunek and H. Ebert, J. Phys.: Condens. Matter **19**, 096203 (2006).
  - <sup>11</sup> R. Robles, A. Bergman, A. B. Klautau, O. Eriksson and L. Nordström J. Phys.: Condens. Matter **20**, 015001 (2008).
  - <sup>12</sup> C. Etz, B. Lazarovits, J. Zabloudil, R. Hammerling, B. Ujfalussy, L. Szunyogh, G. M. Stocks, and P. Weinberger, Phys. Rev. B **75**, 245432 (2007).
  - <sup>13</sup> A. Bergman, L. Nordström, A. B. Klautau, S. Frota-Pessoa, and O. Eriksson Surface Science **600**, 4838 (2006).
  - <sup>14</sup> A. Bergman, L. Nordström, A. B. Klautau, S. Frota-Pessoa, and O. Eriksson J. Phys.: Condens. Matter **19**, 156226 (2007).
  - <sup>15</sup> S. Lounis, Ph. Mavropoulos, P. H. Dederichs, and S. Blügel Phys. Rev. B **72**, 224437 (2005).
  - <sup>16</sup> S. Lounis, Ph. Mavropoulos, R. Zeller, P. H. Dederichs, and Stefan Blügel, Phys. Rev. B **75**, 174436 (2007).
  - <sup>17</sup> S. Lounis, P.H. Dederichs, and S. Blügel, Phys. Rev. Lett. **101**, 107204 (2008).
  - <sup>18</sup> S. Lounis, M. Reif, P. Mavropoulos, L. Glaser, P. H. Dederichs, M. Martins, S. Blügel and W. Wurth Europys. Lett. **81**, 47004 (2008).
  - <sup>19</sup> C. F. Hirjibehedin, C.-Y. Lin, A. F. Otte, M. Ternes, C. P. Lutz, B. A. Jones, and A. J. Heinrich, Science **317**, 1199 (2007).
  - <sup>20</sup> A. F. Otte, M. Ternes, K. von Bergmann, S. Loth, H. Brune, C. P. Lutz, C. F. Hirjibehedin, and A. J. Heinrich, Nature Physics **4**, 847 (2008).
  - <sup>21</sup> C. L. Gao, A. Ernst, G. Fischer, W. Hergert, P. Bruno, W. Wulfhekel, and J. Kirschner, Phys. Rev. Lett. **101**, 167201 (2008).
  - <sup>22</sup> T. Balashov, A. F. Takacs, M. Dane, A. Ernst, P. Bruno, and W. Wulfhekel, Phys. Rev. B **78**, 174404 (2008).
  - <sup>23</sup> F. Meier, L. Zhou, J. Wiebe, and R. Wiesendanger, Science **320**, 82 (2008).
  - <sup>24</sup> J. Minár, S. Bornemann, O. Šipr, S. Polesya, and H. Ebert, Appl. Phys. A **82**, 139 (2006).
  - <sup>25</sup> S. Polesya, O. Šipr, S. Bornemann, J. Minár, and H. Ebert, Europhys. Lett. **74** 1074 (2006).
  - <sup>26</sup> S.H. Vosko, L. Wilk, and M. Nusair, Can. J. Phys. **58**, 1200 (1980).
  - <sup>27</sup> N. Papanikolaou, R. Zeller and P.H. Dederichs J. Phys.: Condens. Matter **14**, 2799 (2002); N. Stefanou, H. Akai, and R. Zeller, Comp. Phys. Commun. **60**, 231 (1990); N. Stefanou and R. Zeller, J. Phys.: Condens. Matter **3**, 7599 (1991).
  - <sup>28</sup> A.I. Liechtenstein, M.I. Katsnelson, V.P. Antropov, and V.A. Gubanov, J. Magn. Magn. Mater. **67** 65 (1987).

- <sup>29</sup> M. Pajda, J. Kudrnovský, I. Turek, V. Drchal, and P. Bruno, Phys. Rev. B **64**, 174402 (2001).
- <sup>30</sup> O. O. Brovko, W. Hergert, and V. S. Stepanyuk Phys. Rev. B **79**, 205426 (2009).
- <sup>31</sup> O. O. Brovko, P. A. Ignatiev, V. S. Stepanyuk, and P. Bruno, Phys. Rev. Lett. **101**, 036809 (2008).
- <sup>32</sup> A. Weismann, M. Wenderoth, S. Lounis, P. Zahn, N. Quaas, R. G. Ulbrich, P. H. Dederichs, and S. Blügel Science **323**, 1190 (2009).
- <sup>33</sup> M. Bode, M. Heide, K. von Bergmann, P. Ferriani, S. Heinze, G. Bihlmayer, A. Kubetzka, O. Pietzsch, S. Blügel, and R. Wiesendanger, Nature (London) **447**, 190 (2007)
- <sup>34</sup> A. Antal, B. Lazarovits, L. Udvardi, L. Szunyogh, B. Ujfalussy, and P. Weinberger, Phys. Rev. B **77**, 174429 (2008).
- <sup>35</sup> S. Mankovsky, S. Bornemann, J. Minar, S. Polesya, H. Ebert, J. B. Staunton, and A. I. Lichtenstein, Phys. Rev. B **80**, 014422 (2009).
- <sup>36</sup> S. Alexander and P. W. Anderson Phys. Rev. **133**, A1594 (1964).
- <sup>37</sup> The same mechanisms appear and compete also in diluted magnetic semiconductors; see, e.g., H. Akai, Phys. Rev. Lett. **81**, 3002 (1998); B. Belhadji, L. Bergqvist, R. Zeller, P.H. Dederichs, K. Sato, and H. Katayama-Yoshida, J. Phys.: Condens. Matter **19**, 436227 (2007).
- <sup>38</sup> Also monoatomic Cr chains show stronger antiferromagnetism than Mn chains. See, e.g., Y. Mokrousov, G. Bihlmayer, S. Blügel, and S. Heinze, Phys. Rev. B **75**, 104413 (2007).
- <sup>39</sup> O. Šipr, private communication.